Secondary ion mass spectrometry analysis of vertical cavity surface-emitting lasers

Yong K. Kim and Kent D. Choquette[a)]
Micro and Nanotechnology Laboratory, University of Illinois at Urbana–Champaign, Urbana, Illinois 61801

Judith E. Baker
The Frederick Seitz Materials Research Laboratory, University of Illinois at Urbana–Champaign, Urbana, Illinois 61801

Andrew A. Allerman
Sandia National Laboratories, Albuquerque, New Mexico 87185

(Received 29 October 2003; accepted 1 March 2004; published 26 April 2004)

Depth profile analysis by high-resolution secondary ion mass spectrometry (SIMS) can accurately determine C and Si concentrations within monolithic reflectors of vertical cavity surface-emitting lasers (VCSELs). These SIMS depth profiles are quantified to atomic concentrations using relative sensitivity factors and calibration standards, and are correlated to the laser characteristics. We compare the light output versus current and voltage of a conventional oxide-confined VCSEL with a self-pulsating VCSEL. We show that SIMS depth profiling of VCSELs can be useful as a diagnostic method for VCSEL epitaxial wafers, and that the doping level of oxide aperture layers can dramatically impact the device performance. © *2004 American Vacuum Society.*
[DOI: 10.1116/1.1715051]

I. INTRODUCTION

Secondary ion mass spectrometry (SIMS) has proven to be a versatile analysis technique for measuring doping profiles of semiconductor materials because it can detect impurities and dopants at extremely low atomic concentrations of less than one part per million.[1] The secondary ion counts from SIMS measurements can be quantified to atomic concentration by using relative sensitivity factors (RSFs)[2] for typical impurity elements in GaAs materials. These SIMS depth profiles provide valuable information for the development of semiconductor epitaxial structures and the analysis of device performance. The epitaxial structure of a vertical cavity surface-emitting laser (VCSEL) is quite complex, requiring as many as 100 distinct layers with stringent tolerances on composition, thickness, and doping concentration.[3] Optical reflectance characterization can provide a wealth of information regarding the thickness and composition, but the sophisticated doping profiles required to enable low series resistance and to minimize free-carrier absorption in VCSELs are difficult to determine.[4,5] Depth profile analysis by high-resolution mode SIMS is an effective technique to determine C and Si doping concentration. Quantified depth profiles determined from RSF, can be useful when analyzing laser performance characteristics, such as light output versus current and voltage. In this article, an oxide-confined VCSEL and a self-pulsating oxide-confined VCSEL[6] are examined in order to evaluate the correlation between SIMS depth profiles and device performance.

[a)]Electronic mail: choquett@uiuc.edu

II. EXPERIMENT

The basic device structure of an 850 nm VCSEL consists of an active cavity containing multiple GaAs quantum wells, and *p*- and *n*-type-doped distributed Bragg reflectors (DBRs), all of which are grown by metalorganic vapor phase epitaxy (MOVPE). The cross section of a VCSEL is schematically shown in Fig. 1. The DBR mirrors are comprised of repeating periods of $Al_{0.16}Ga_{0.84}As/Al_{0.92}Ga_{0.08}As$ layers doped with parabolic compositional grading at the interfaces. For the *p*- and *n*-type mirrors, C and Si dopants are used, respectively. In order to achieve lateral confinement of both the optical mode and current, $Al_{0.98}Ga_{0.02}As$ layers adjacent to the active region are incorporated. These high Al content layers are used to form buried oxide apertures by selective wet oxidation after mesa etching.

The doping concentrations in VCSEL epiwafers are measured by high mass resolution mode SIMS. The SIMS analyses are performed by using a CAMECA IMS-5f with a 14.5 keV Cs+ primary ion beam and negative secondary ion detection. A primary ion beam is scanned over an area of $150 \times 150\ \mu m^2$. Negatively charged secondary ions are collected from a circular area of 30 μm diameter at the center of the primary ion raster area. Six different single elements are detected, such as ^{12}C and ^{28}Si for dopants, ^{27}Al, ^{69}Ga, and ^{75}As for matrix elements, and ^{16}O as reference. A Cs+ primary ion beam is employed during these measurements because high-energy Cs+ ions will increase the yield of negative secondary ions, especially for the ^{12}C and ^{28}Si.[2] Moreover, secondary ion counts of these single elements are quantifiable within the GaAs matrix using RSFs. (In contrast, the RSF values of ^{27}Al, ^{69}Ga, and ^{75}As are not reliable to quantify the atomic concentrations using the Cs+ primary ion beam,[2] although the relative variations of these matrix ele-

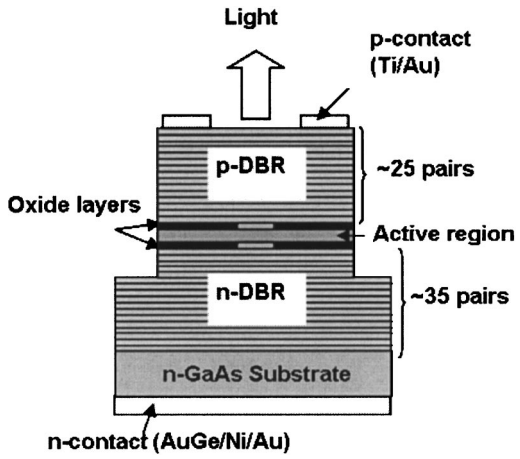

FIG. 1. Schematic cross-section diagram of an oxide VCSEL.

ments are sufficient for our purpose of interpretation of the VCSEL epitaxial structure.)

In order to obtain precise depth distributions and avoid mass interference between ^{28}Si, $^{27}Al-^{1}H$, and $^{12}C-^{16}O$ compounds, high mass resolution mode measurements are carried out. Mass interference can occur because the masses of both Al–H (27.98936 amu), and C–O (27.99491 amu) compounds are nearly equal to the mass of Si (27.97693 amu). Without accounting for these interferences, the Si concentration would be overestimated. The calibrated RSF values of C and Si are confirmed from SIMS depth profiles of standard samples with several different Al compositions and known impurity concentrations.

Since SIMS analyses can only determine atomic concentrations, the relationship between atomic and carrier concentration for each Al composition layer must be determined. We measure the atomic concentration by SIMS of several reference samples, in which carrier concentrations are known by other methods. These 1000 nm thick reference samples for carrier concentration calibration are grown on undoped AlGaAs buffer layers on semi-insulating GaAs substrates, thereby preventing carriers from transporting to the GaAs/AlGaAs interface. The electronic carrier concentrations are measured by Polaron capacitance–voltage or Hall measurements. The ratio of the carrier concentration to doping concentration represents the proportion of electronically activated impurities in the material. The SIMS depth profiles from VCSEL epitaxial wafers are used to study how differences in impurity concentrations affect laser characteristics, such as light output versus current and voltage.

III. RESULTS AND DISCUSSION

The SIMS depth profiles of a conventional oxide VCSEL are plotted in Figs. 2 and 3. Figure 2 shows the uncalibrated secondary ion counts of six different elements detected by high mass resolution mode SIMS. Figure 3 presents the calibrated doping concentration of C and Si near the active region of the VCSEL. The measured secondary ion counts maintain sufficient depth resolution down to 4 μm sputtering depth, which is sufficient to determine the epitaxial VCSEL

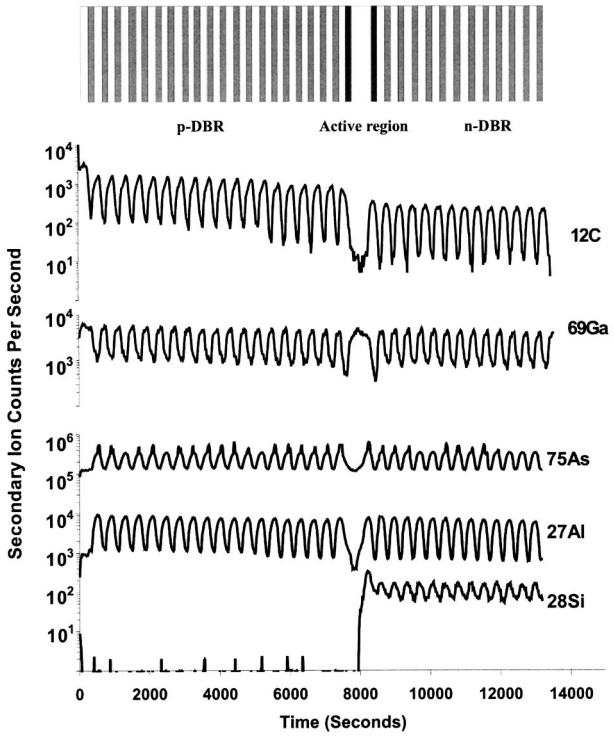

FIG. 2. Secondary ion counts measured from a VCSEL wafer with a schematic of the epitaxial structure of an oxide VCSEL. The darker layers in the DBRs represent the layers with higher Al concentration.

structure. The secondary ion counts of As and Al oscillate in phase in Fig. 2 because the secondary ion yields in $Al_{0.92}Ga_{0.08}As$ are larger than those in $Al_{0.16}Ga_{0.84}As$ due to matrix effects.[2] The high C concentration ($\sim 5\times 10^{19}$) observed in the top p-DBR layer enables a p-type ohmic contact with a Ti/Au metalization.

The C concentration in Fig. 3 varies by a factor of 10 depending on Al composition in the DBR layers. During MOVPE, carbon tetrachloride (CCl_4) gas is used as the C doping precursor. The carbon atoms are incorporated into the As sites at the growth surface. However, this precursor gas also produces an etch-back reaction due to the presence of Cl reactants.[7] During the etch-back reaction, $GaCl_3$ is the more volatile product than $AlCl_3$. Thus, as the Al composition increases with constant CCl_4 flow, the etch-back rate de-

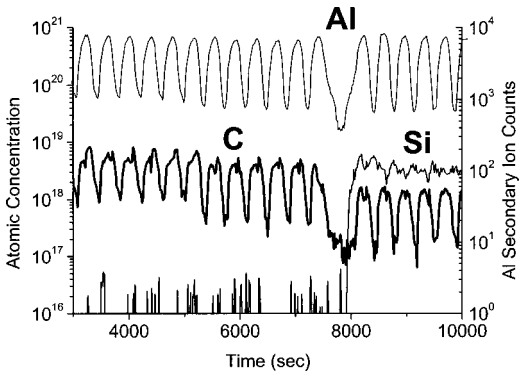

FIG. 3. Quantified depth profile near the active region of an oxide VCSEL.

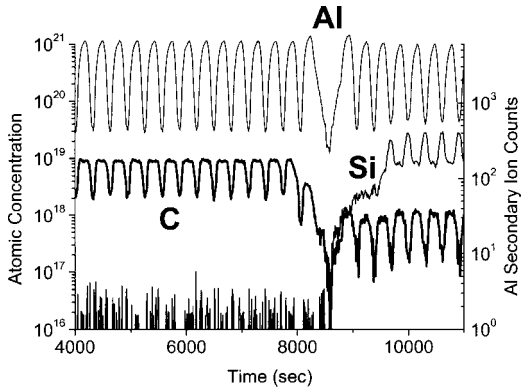

FIG. 4. Quantified depth profile near the active region of a self-pulsation VCSEL.

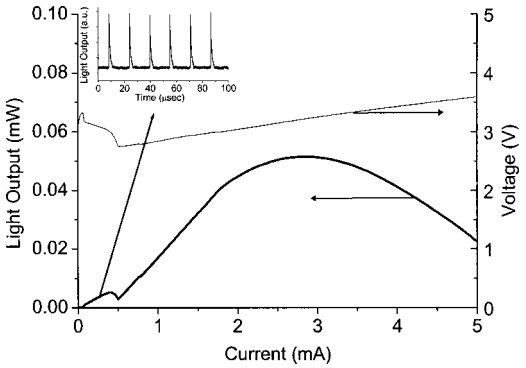

FIG. 5. Light output characteristics of an oxide VCSEL and a self-pulsating VCSEL. Inset represents a self-pulsating phenomenon under very low current injection.

creases, resulting in more carbon incorporation into As sites. Furthermore, since the Al—C bond energy (65 kcal/mol) is larger than Ga—C bond energy (59 kcal/mol),[8] carbon doping in high Al layers is thermodynamically more favorable than in low Al layers. In the *n*-type DBR layers, di-silane (Si_2H_6) gas is used as the Si source for doping. This precursor gas does not have a strong compositional dependency on the Al composition, and lacks an etch-back behavior. Therefore, the Si concentration curve does not fluctuate as much as the C concentration in *n*-type DBR region as apparent in Fig. 3. Finally, as noted in Fig. 3, the five *p*-DBR pairs nearest to the active region are lower doped with carbon to reduce the free-carrier absorption near the optical cavity where the optical field has its greatest amplitude.

Figure 4 shows the quantified depth profile of an oxide-confined VCSEL which displays self-pulsating operation.[6] In Fig. 4, the C doping profile is nearly the same as that in conventional oxide VCSEL shown in Fig. 3. However, the Si concentration curve shows two abnormal behaviors. First, the Si concentration in the *n*-type oxide layer is approximately equal to the C concentration in that layer. The background carbon in the *n*-type layers is obtained from the MOVPE gas precursors. The background C concentrations of *n*-DBR layers are in the range of 1×10^{17} to 1×10^{18} as shown in Figs. 3 and 4. This implies the Si concentration in the *n*-type oxide layer is insufficient to compensate for the background carbon in Fig. 4. We also note that *n*-type DBR layers are extremely heavily doped with Si ($\sim1\times10^{19}$) in Fig. 4.

For the VCSEL analyzed in Fig. 4, the self-pulsating operation is manifest as laser pulsations under very low direct current (dc) injection.[6] The light output characteristics versus current and voltage of a self-pulsating VCSEL is shown in Fig. 5. From the light output characteristics and the SIMS depth profile of a self-pulsation VCSEL, the self-pulsation phenomenon can be explained by the following model. A very lightly doped *n*-type oxide aperture layer acts as a barrier in conduction band. Since electrons are injected into the active region through this oxide aperture by thermionic emission, insufficient injection under low dc bias results in self-pulsating. We also observe negative differential resistance at the injection currents where self-pulsating occurs in Fig. 5. Eventually, continuous wave operation occurs under a high enough bias in Fig. 5.

Table I summarizes the relationship between doping concentration and carrier concentration. This information is required to directly correlate SIMS analysis and device performance. In Table I, carrier concentration calibration samples are measured by Polaron or Hall measurement for low and high Al composition AlGaAs layers. The average atomic concentrations from SIMS depth profiles show doping concentrations of the samples. In the last column, the ratio of Polaron to SIMS represents how many dopants are electronically activated in the matrix. From Table I, we can confirm that approximately 80% of both Si and C are electronically activated regardless of Al composition. Therefore, SIMS depth profiles can be directly used to understand device performance without further calibration.

IV. CONCLUSION

We have shown that high-resolution mode SIMS can accurately determine the doping profiles in the epitaxial structure of VCSELs. The control of doping concentration in VCSELs is very important for achieving low series resistance, while simultaneously maintaining minimal free-carrier absorption. We find that the C concentrations in the DBR layers are strongly dependent on Al composition with background C level in *n*-DBR layers ranging from 1×10^{17} to 1×10^{18}. Thus, the *n*-type oxide layer should be sufficiently doped with Si to compensate for the background C. When this is

TABLE I. Doping concentration versus carrier concentration for various reference samples.

Dopant	Polaron/Hall	SIMS	Al %	Ratio (Polaron/SIMS)
C	6.90×10^{17}	7.90×10^{17}	10%	0.873
C	1.88×10^{18}	3.00×10^{18}	16%	0.627
C	3.27×10^{18}	4.12×10^{18}	92%	0.794
Si	2.10×10^{18}	2.70×10^{18}	16%	0.778
Si	1.53×10^{18}	1.89×10^{18}	16%	0.810
Si	5.04×10^{18}	6.20×10^{18}	92%	0.812

not the case, particularly in the oxide aperture layer, unusual laser operation, such as self-pulsating, can occur. Therefore, as seen from our results, accurate determination of doping profiles using SIMS characterization of VCSEL wafers can serve as a valuable tool to understand the laser performance.

ACKNOWLEDGMENTS

This work was partially support by the Defense Advanced Research Projects Agency under Award No. 317271-7830. SIMS measurements were carried out in the Center for Microanalysis of Materials, University of Illinois, which is partially supported by the U.S. Department of Energy under Grant No. DEFG02-91-ER45439.

[1]J. C. Vickerman, A. Brown, and N. M. Reed, *Secondary Ion Mass Spectrometry: Principles and Applications* (Oxford University Press, New York, 1989).
[2]R. G. Wilson, F. A. Stevie, and C. W. Magee, *Secondary Ion Mass Spectrometry: A Practical Handbook for Depth Profiling and Bulk Impurity Analysis* (Wiley, New York, 1987).
[3]C. Wilmsen, H. Temkin, and L. A. Coldren, *Vertical-Cavity Surface-Emitting Lasers: Design, Fabrication, Characterization, and Applications* (Cambridge University Press, New York, 1999).
[4]J. F. Zheng, D. F. Ogletree, J. Walker, M. Salmeron, and E. R. Weber, J. Vac. Sci. Technol. B **12**, 2100 (1994).
[5]A. Khan, K. Woodbridge, M. Ghisoni, G. Parry, G. Beyer, J. Roberts, M. Pate, and G. Hill, J. Appl. Phys. **77**, 4921 (1995).
[6]K. D. Choquette, H. Q. Hou, K. L. Lear, H. C. Chui, K. M. Geib, A. Mar, and B. E. Hammons, Electron. Lett. **32**, 459 (1996).
[7]H. Q. Hou, B. E. Hammons, and H. C. Chui, Appl. Phys. Lett. **70**, 3600 (1997).
[8]A. C. Jones, J. Cryst. Growth **129**, 728 (1993).